



Hydrogenation rate limiting step, diffusion and thermal conductivity in cold rolled magnesium hydride



Julien Lang^{a,*}, Mitch Eagles^b, Mark S. Conradi^b, Jacques Huot^a

^aHydrogen Research Institute, Université du Québec à Trois-Rivières, 3351 des Forges, Trois-Rivières, Québec G9A 5H7, Canada

^bWashington University, Dept. of Physics, 1105, One Brookings Drive, Saint Louis, MO 63130, USA

ARTICLE INFO

Article history:

Received 3 May 2013

Received in revised form 14 August 2013

Accepted 20 August 2013

Available online 30 August 2013

Keywords:

Metal hydrides

Hydrogen absorbing materials

Kinetics

Thermal analysis

Nuclear resonances

ABSTRACT

In this paper, the investigation of the rate limiting steps in hydrogen absorption and desorption of cold rolled magnesium hydride is reported. Absorption and desorption curves were made at different temperatures with constant driving force. Results show that the rate limiting step of the reactions of magnesium with hydrogen does not change with temperature. After cold rolling, hydrogen absorption is diffusion controlled, while the desorption process is three dimensional growth of existing nuclei. NMR measurements are also reported; there is no increase in the rate of hydrogen diffusive motions in the cold rolled material, compared to bulk. The effect of rolling and ball milling on thermal conductivity was also investigated.

© 2013 Elsevier B.V. All rights reserved.

1. Introduction

Despite its high hydrogen storage capacity, magnesium hydride is difficult to use in practical hydrogen storage applications because of its high temperature of operation and slow kinetics. Recently, it has been shown that severe plastic deformation (SPD) techniques can enhance hydrogen sorption kinetics of magnesium and magnesium-based hydrides [1–9].

Leiva et al. have investigated the effect of SPD using techniques such as high pressure torsion (HPT), cold rolling, and forging on MgH₂ and MgH₂–Fe mixtures [10]. They found that SPD reduces the crystallite size and, similar to ball milling, can also produce the high pressure high temperature γ -MgH₂ phase. This means that for magnesium hydride, SPD methods can be considered as replacements for the ball milling technique. In a previous investigation, we have reported the effect of cold rolling on MgH₂'s morphology, crystallography and hydrogen sorption kinetics [11]. We found that five rolling passes are equivalent to 30 min of high energy milling in terms of hydrogen sorption enhancement while using significantly less energy. Thus, cold rolling may be important in “activating” magnesium hydride for large-scale hydrogen storage applications, where the energy required for ball-milling becomes prohibitive.

To get a better understanding of the effect of cold rolling on magnesium hydride, we investigated the rate limiting step, nuclear

magnetic resonance and thermal conductivity. Cold rolling MgH₂ for five rolling passes enhances the hydrogen absorption properties so that they are equivalent to the result of 30 min of high energy ball milling [11]. The present investigation will give a better understanding of the differences between cold rolling and ball milling of MgH₂ powder on the hydrogenation mechanism (rate limiting step). We also examined the changes in thermal conductivity upon cold rolling, because thermal conduction can be rate limiting in absorption and desorption of large hydride beds. Finally, hydrogen NMR was used to determine whether cold rolling enhances the rate of hydrogen atomic diffusive motions in MgH₂.

2. Experimental methods

The cold-rolling apparatus used in this study was a Durston DRM 100 modified in order to have the sample pass vertically through the rollers. This configuration enables easy processing of powders. The apparatus' stainless steel rollers have a diameter of 6.5 cm and a length of 13 cm. The driving motor is a 1.1 kW Rossi Motoriduttori DC electric motor. For the rolling experiment, 300-mesh MgH₂ powder (98% purity), provided by Alfa Aesar, was inserted in between two 1 mm thick 316 stainless steel plates and rolled. New stainless steel plates were cleaned with alcohol prior to each experiment in order to protect the rollers and samples from cross-contamination. Cold rolling magnesium hydride powder consolidates the powder and changes its morphology to thin plate. The MgH₂ plate thicknesses vary from 0.3 to 0.8 mm. They were collected and rolled again to the desired number of rolling passes. For this study, the samples were cold rolled a total of five times before characterization.

Hydrogen absorption and desorption data were gathered using a homemade Sieverts type PCT apparatus (pressure, composition, temperature). Absorption and desorption kinetics were performed at temperatures of 573, 598, 623, and 648 K while keeping the driving force constant. The driving force, F_d for absorption and

* Corresponding author. Tel.: +1 819 376 5011x3581.

E-mail address: julien.lang@uqtr.ca (J. Lang).

Table 1
Experimental conditions for absorption and desorption at different temperatures.

Temperature (K)	Absorption pressure (kPa)	Desorption pressure (kPa)	Equilibrium pressure (kPa)
573	675	49	183
598	1205	100	352
623	2050	195	640
648	3360	365	1113

F_d for desorption, is a function of the ratio of the reaction's equilibrium pressure and the applied H_2 pressure. Since the reaction's equilibrium pressure varies with temperature, the applied pressure should also change with temperature. According to Rudman, the driving forces for absorption and desorption are respectively given by [17]:

$$F_a = T[1 - \sqrt{(P_e/P)}]$$

and

$$F_d = T[1 - \sqrt{(P/P_e)}]$$

where F represents the driving force, T is the temperature of the experiment, P_e is the equilibrium pressure, and P is the applied H_2 pressure. The equilibrium pressures were taken from the DOE metal hydride data base [18]. In this investigation, the driving force (F) was kept constant at a value of 275 for both absorption and desorption. Table 1 presents the absorption and desorption applied pressures giving a driving force of 275 for the temperatures used in this investigation.

The shape of the absorption and desorption curves are controlled by the slowest process in the reactions, the rate limiting step. The absorption and desorption reactions' rate limiting steps were determined using the experimental raw data files and plotting the hydrogen uptake ratio ($X = \%H_{abs}/\%H_{max}$) into the known models developed by Mintz et al. and Avrami [13,14]. Linear regressions were performed on the resulting curves; the model with the best fit to the data then represents the reaction's rate limiting step.

Thermal conductivity was measured using a TCI C-Therm Thermal Analyser. As-received MgH_2 powder was measured with the apparatus' loose powder mode. This was compared with the measurement of MgH_2 that had been cold rolled five times and subsequently reduced to a powder in a mortar and pestle. Thermal conductivity of a compressed pellet, to simulate cold rolled MgH_2 plates, was also measured.

NMR measurements were performed on the cold rolled samples. Loaded into glass tubes for NMR in a N_2 -atmosphere glove bag, the NMR samples (~0.2 g) and flame sealed into glass tubes approximately 5 mm OD, 4 mm ID, and 20 cm long with 0.9 bar N_2 gas.

The NMR apparatus was a home-built pulsed superheterodyne with quadrature phase detection and 4-phase transmitter. The final transmitter output power was 25 W. A pulse generator based on the Pulse Blaster card provided automation of pulse sequences, particularly for measuring relaxation times. An iron-core Varian XL-100 magnet provided 2.0 T (H frequency of 85.03 MHz) with F-19 NMR field stabilization. The NMR probe was a rectangular aluminum box fitting the magnet gap with tuning components at room temperature. The rf coil and sample were immersed in a 50 L per minute stream of temperature-regulated air in a vacuum-insulated Dewar tube. Temperatures were measured with a type-T thermocouple approximately 2 cm from the sample. Line shapes were obtained by Fourier transforming the free induction decays (FID), being careful to minimize the receiver dead time following the rf pulse (the dead time was reduced to about 2 μs by means of a low-Q rf probe circuit). The dead time data were replaced by extrapolating the latter-time data back to the end of the rf pulse. Because of the low transmitter power, the $\pi/2$ pulse time was typically 10 μs . Thus, good line shapes were obtained using 1 or 2 μs excitation pulses to minimize relaxation and dephasing during the rf pulse.

The decay time T_{1D} of dipolar spin-order was measured with the Jeener–Broekaert sequence: $(\pi/2)_{x-x} - t - (\pi/4)_y - \tau - (\pi/4)$ -acquire. The time t was chosen to generate the largest amplitude Jeener echo following the third pulse; the optimum t was very short at 2 μs , because of the long rf pulses used. The first pulse was phase-cycled ($x, -x$) and data were acquired in the receiver with cycling (add, subtract). The Jeener echo amplitude A was fitted to $A \sim \exp(-\tau/T_{1D})$ to obtain T_{1D} . We were always careful to be on-resonance to within a very small fraction of the 50 kHz line width. The laboratory-frame T_1 was determined by the saturate-wait-inspect strategy. The saturation sequence used ten $\pi/2$ rf pulses separated by 1 ms each; the inspection sequence was a single $\pi/2$ pulse followed by the acquired FID.

3. Results and discussion

3.1. Rate limiting step

The absorption and desorption curves used to identify the rate limiting step in cold rolled MgH_2 are presented in Figs. 1 and 2

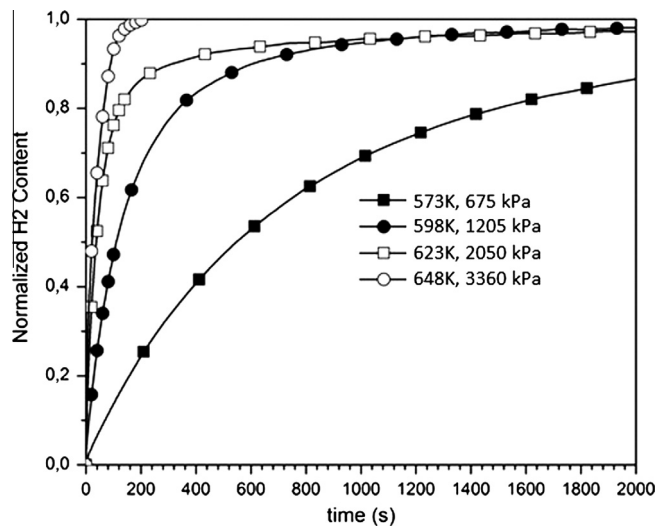


Fig. 1. Cold rolled MgH_2 absorption curves. The smooth curves simply connect the data points.

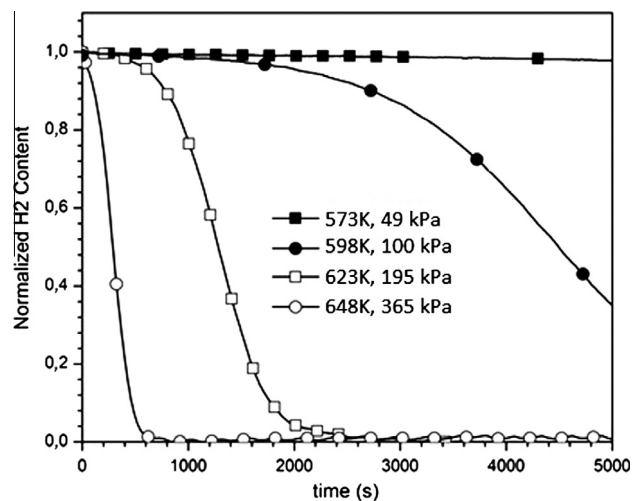


Fig. 2. Cold rolled MgH_2 desorption curves. The smooth curves simply connect the data points.

respectively. It is clear that raising the temperature while keeping the driving force constant greatly enhances the sorption kinetics. For the desorption curves shown in Fig. 2, raising the temperature also diminishes the desorption incubation time. All the samples were found to have the same rate-limiting step; we present here the details of only the measurements at 623 K.

As shown in the literature, different reaction mechanisms are represented by different equations [13,14]. The models tested in this study are presented in Table 2. The left side of the equations is a function solely of the reaction's completion ratio (X). In the present case, the absorption ratio is given by the absorbed quantity of hydrogen in the sample divided by the sample's maximum absorption capacity. To find the correct rate-limiting step, we plotted the left side of these equations as a function of time. For this kind of plot, the correct rate-limiting step will be the one giving a linear curve. Fig. 3 shows this type of plot for absorption at 623 K. Linear regressions were performed on each model. Barkhordarian et al., calculated the linear regressions from 20% to 80% of the reaction's completion ($X = [0.2 \dots 0.8]$) [12]. We chose to calculate our regressions from 10% to 90% of the reaction's completion ($X = [0.1 \dots 0.9]$) to get a wider range of the reaction fitted while

Download English Version:

<https://daneshyari.com/en/article/1612735>

Download Persian Version:

<https://daneshyari.com/article/1612735>

[Daneshyari.com](https://daneshyari.com)